Physica A 392 (2013) 149–156

Contents lists available at SciVerse ScienceDirect

Physica A

journal homepage: www.elsevier.com/locate/physa

Percolation of dimers on square lattices

W. Lebrecht [a], J.F. Valdés [a], E.E. Vogel [a], F. Nieto [b], A.J. Ramirez-Pastor [b,*]

[a] Departamento de Física, Universidad de La Frontera, Casilla 54-D, Temuco, Chile

[b] Dpto. de Física, Instituto de Física Aplicada, Universidad Nacional de San Luis - CONICET, Ejército de los Andes 950, 5700 San Luis, Argentina

ARTICLE INFO

Article history:
Received 29 June 2012
Received in revised form 14 August 2012
Available online 25 August 2012

Keywords:
Percolation
Multisite occupancy
Critical exponents
Scaling phenomena

ABSTRACT

A theoretical approach, based on exact calculations of configurations on finite rectangular cells, is applied to study the percolation of homonuclear dimers on square lattices. An efficient algorithm allows us to calculate the detailed structure of the configuration space for $M = L_x \times L_y$ cells, with M varying from 16 to 36. The percolation process has been monitored by following the percolation function, defined as the ratio between the number of percolating configurations and the total number of available configurations for a given cell size and concentration of occupied sites. The percolation threshold has been calculated by means of two complementary methods: one based on well-known renormalization techniques and the other based on determining the inflection point of the percolation function curves. A comparison of the results obtained by these two methods has been performed. The study includes the use of finite-size scaling theory to extrapolate numerical results towards the thermodynamic limit. The effect of jamming due to dimers is also established. Finally, the critical exponents ν, β and γ have been obtained and values compared with numerical results and expected theoretical estimations. The present results show agreement and even improvement (in the case of γ) with respect to some numeric values available in the literature.

1. Introduction

The percolation problem is a topic being increasingly considered in statistical physics. One reason for this current interest is that it is clear that generalizations of the pure percolation problem are likely to have extensive applications in science and technology [1–5]. Although it is a purely geometric phenomenon, the phase transition involved in the process can be described in terms of a usual continuous phase transition. This mapping to critical phenomena has made percolation a full part of the theoretical framework of collective phenomena and statistical physics.

In this context, percolation of monomers (particles occupying one lattice site each) has been one of the most studied models in the literature, and the corresponding percolation threshold p_c has been measured to high precision for decades [6–10]. The problem becomes considerably difficult when some sort of correlation exists, such as particles that occupy several k contiguous lattice sites (k-mers). Consequently, there have been fewer studies devoted to the problem of percolation of structured objects. Among them, Leroyer and Pommiers [11] studied the percolation behavior of a random sequential adsorption (RSA) of linear segments with different sizes, and Gao and Yang [12] and Cherkasova et al. [13] analyzed the percolation of dimers. In all cases, the dependence of the percolation threshold on the parameters of the problem and the universality of the phase transition have been discussed. However, Ref. [11] is limited due to finite-size effects, while Refs. [12,13] are just restricted to the case $k = 2$ (dimers). In fact, Leroyer and Pommiers found that, as the

* Corresponding author.
E-mail address: antorami@unsl.edu.ar (A.J. Ramirez-Pastor).

0378-4371/$ – see front matter © 2012 Elsevier B.V. All rights reserved.
doi:10.1016/j.physa.2012.08.014

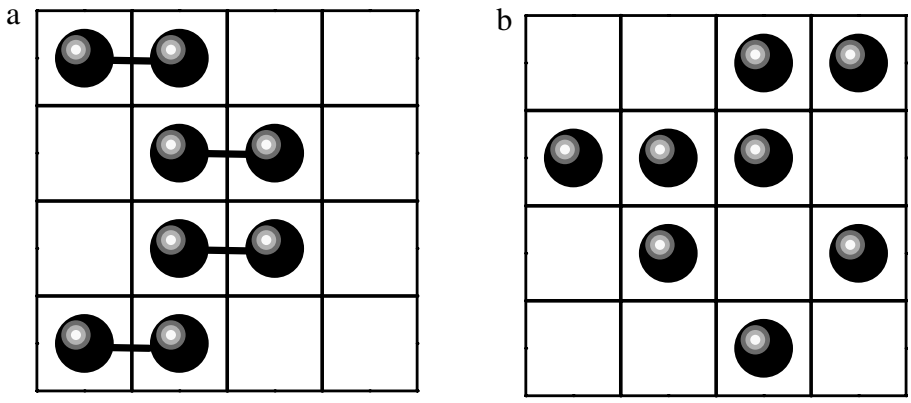

Fig. 1. (a) Snapshot corresponding to one of the possible configurations for a system of four dimers on a 4×4 cell. Full circles and empty squares represent dimer units and empty sites, respectively. (b) As part (a) for a system of eight monomers on a 4×4 cell. Full circles and empty squares represent monomers and empty sites, respectively.

segment length grows, the percolation threshold decreases, goes through a minimum, and then increases slowly for large segments. Further studies by Cornette et al. [14] showed a monotonic dependence of the percolation threshold on the size of the deposited element, in contrast with the results of Ref. [11]. This discrepancy was explained because of the finite-size effect not being considered in Ref. [11].

As discussed in the previous paragraph, it took until 2003 to elucidate the dependence of p_c on k for tortuous and rigid k-mers deposited according to an RSA process. In addition, the phase transition predicted by Monte Carlo (MC) techniques in Refs. [11–14] has not been corroborated yet by analytical methods. In this framework, the main objective of the present work is, using an analytical technique, to determine the full set of characteristic parameters of percolation (percolation threshold and critical exponents) for a system of dimers, randomly and irreversibly deposited on a square lattice.[1] We make use of the opportunity of considering the effect of jamming on the coverage of square lattices upon using dimers. The study is based on (i) exact calculation of configurations on finite $M = L_x \times L_y$ cells, with M varying from 16 to 36 and (ii) the use of finite-size scaling techniques [15–17].

The rest of the paper is organized as follows. In Section 2, the theoretical formalism is presented. The analysis of the results and discussion are given in Section 3. Finally, the conclusions are drawn in Section 4.

2. Theory

In the filling process, rigid dimers are deposited sequentially and irreversibly on an initially empty square cell of $M = L_x \times L_y$ sites with the following restrictions: (1) the depositing objects contain two identical units; (2) the distance between dimer units is assumed in registry with the lattice constant a; hence exactly two sites are occupied by a dimer when deposited; (3) the incoming particles must not overlap with previously added objects; and (4) the elements remain frozen in the lattice. In any case, the procedure is iterated until N dimers are placed on the cell and the desired concentration (given by $p = 2N/M$) is reached. A configuration is a distribution of empty and occupied sites on the cell. Fig. 1(a) shows one of the possible configurations corresponding to a system of four dimers on a 4×4 cell. In part (b), one possible configuration of monomers at the same concentration as that in part (a) is plotted. Note that the configuration in part (b) is not available for dimers. Thus, not all the available configurations of empty and occupied sites can be reached by dimer deposition.

A central idea of percolation theory is based on finding the minimum concentration p for which a cluster (a group of occupied sites in such a way that each site has at least one occupied nearest-neighbor site) extends from one side of the system to the opposite one. This particular value of the concentration rate is named the critical concentration or percolation threshold p_c, and it determines a phase transition in the system. In the monomeric random percolation model, any single site (or a bond connecting two sites) is occupied with probability p. For the precise value of p_c, the percolation threshold of sites (bonds), at least one spanning cluster connects the opposite borders of the system (indeed, there exists a finite probability of finding n (> 1) spanning clusters [18–21]). In that case, a continuous phase transition appears at p_c which is characterized by well-defined critical exponents.

Let us define $p(t)$ as the fraction of lattice sites covered at time t by the deposited objects. Due to the blocking of the lattice by the already randomly adsorbed elements, the limiting or jamming coverage, $p^j = p(t \to \infty)$, is less than that corresponding to close packing ($p^j < 1$). Consequently, p ranges from 0 to p^j for objects occupying more than one site. An extensive overview of this field can be found in the excellent work by Evans [22] and the references therein. In the case of

[1] The dimer is the simplest case of a polyatomic adsorbate, and it contains all the properties of multisite-occupancy adsorption.

Table 1
Values of ℓ^{mon}, T_ℓ^{mon} and C_ℓ^{mon} (as indicated in the text) for a system of monomers on a 4×4 cell.

Percolating trajectory, ℓ^{mon}	Polynomial	T_ℓ^{mon}	C_ℓ^{mon}
0	$(1-p)^{16}$	1	0
1	$p(1-p)^{15}$	16	0
2	$p^2(1-p)^{14}$	120	0
3	$p^3(1-p)^{13}$	560	0
4	$p^4(1-p)^{12}$	1820	4
5	$p^5(1-p)^{11}$	4368	60
6	$p^6(1-p)^{10}$	8008	390
7	$p^7(1-p)^9$	11440	1452
8	$p^8(1-p)^8$	12870	3416
9	$p^9(1-p)^7$	11440	5272
10	$p^{10}(1-p)^6$	8008	5414
11	$p^{11}(1-p)^5$	4368	3736
12	$p^{12}(1-p)^4$	1820	1752
13	$p^{13}(1-p)^3$	560	560
14	$p^{14}(1-p)^2$	120	120
15	$p^{15}(1-p)$	16	16
16	p^{16}	1	1

dimers on square lattices, $p^j \approx 0.907$ [13,23,24]. More recently, interesting results have been presented in Refs. [13,23–30], treating the relationship between the jamming coverage and the percolation threshold.

In this paper, the percolation is measured along the x-axis, and symmetric ($L_x = L_y$) and asymmetric ($L_x \neq L_y$) cells are used in the calculations. The percolation trajectory ℓ is defined as the number of objects belonging to the percolating cluster. Thus, the minimum percolation trajectory, represented by $\ell_{\min}$, corresponds to the direct percolation path from left to right (or vice versa), with $\ell_{\min} = L_x$ and $L_x/2$ for monomers and dimers, respectively (when L_x is even). On the other hand, the maximum percolation trajectory, represented by $\ell_{\max}$, corresponds to the number of objects in the saturated cell, with $\ell_{\max} = M$ and $M/2$ for monomers and dimers, respectively (when M is even). In general, the length of a percolation trajectory varies between $\ell_{\min}$ and $\ell_{\max}$.

In the case of monomers, the probability of percolation for any given cell considers the addition of the individual probabilities of all percolating trajectories leading to a polynomial function $f^{mon}_{\ell_{\min},\ell_{\max}}(p)$, where $\ell_{\min} = L_x$ determines the minimum degree of the polynomial function, and $\ell_{\max} = M$ corresponds to the maximum degree associated to it. Then,

$$f^{mon}_{\ell_{\min},\ell_{\max}}(p) = \sum_{\ell=\ell_{\min}}^{\ell=\ell_{\max}} C_\ell^{mon}\, p^\ell (1-p)^{\ell_{\max}-\ell}, \tag{1}$$

where the coefficients C_ℓ^{mon} correspond to the totality of the trajectories of length ℓ leading to percolation. As an example, Table 1 shows the coefficients corresponding to the polynomial function $f^{mon}_{\ell_{\min},\ell_{\max}}(p)$ for a system of monomers on a 4×4 cell. Table 1 also includes the coefficients T_ℓ^{mon}, corresponding to the total number of available configurations for ℓ monomers on the cell.

The counting is more complex in the case of dimers. As mentioned in the first paragraph of this section, not all the available configurations of empty and occupied sites can be reached by dimer deposition. Then, the function f in Eq. (1) must be normalized with a term involving the number of available configurations for dimers on the cell. In this way, the percolating function for dimers can be written as

$$f^{dim}_{\ell_{\min},\ell_{\max}}(d) = \frac{\sum_{\ell=\ell_{\min}}^{\ell=\ell_{\max}} C_\ell^{dim} d^\ell (1-d)^{\ell_{\max}-\ell}}{\sum_{\ell=0}^{\ell=\ell_{\max}} T_\ell^{dim} d^\ell (1-d)^{\ell_{\max}-\ell}}, \tag{2}$$

where $\ell_{\min} = L_x/2$, $\ell_{\max} = M/2$, and $d = p^2$ is the probability of having simultaneous occupation of two neighboring sites. The coefficients C_ℓ^{dim} and T_ℓ^{dim} can be calculated exactly for any given geometry by means of computer algorithms. As the size of the cells expands, the computation of all possible percolating transitions becomes extremely time consuming, which imposes a limitation on the size of the cells to be reached for exact calculations. Table 2 shows the results of this procedure for a 4×4 cell.

In order to compare the data collected in Tables 1 and 2, Fig. 2 presents the curves of C_ℓ^{mon} versus T_ℓ^{mon} (solid symbols) and C_ℓ^{dim} versus T_ℓ^{dim} (open symbols) for different values of length of the percolating trajectories as indicated. Two regimes can be clearly identified: (i) for small and intermediate values of ℓ, the number of percolating configurations of monomers is larger than the corresponding value for dimers (as an example, this is shown in detail in the inset of Fig. 2 for a 4×4 cell);

Table 2
Same as Table 1 for the case of dimers.

Percolating trajectory, ℓ^{dim}	Polynomial	T_ℓ^{dim}	C_ℓ^{dim}
0	$(1-d)^8$	1	0
1	$d(1-d)^7$	24	0
2	$d^2(1-d)^6$	224	4
3	$d^3(1-d)^5$	1044	138
4	$d^4(1-d)^4$	2593	1068
5	$d^5(1-d)^3$	3388	2596
6	$d^6(1-d)^2$	2150	2074
7	$d^7(1-d)$	552	552
8	d^8	36	36

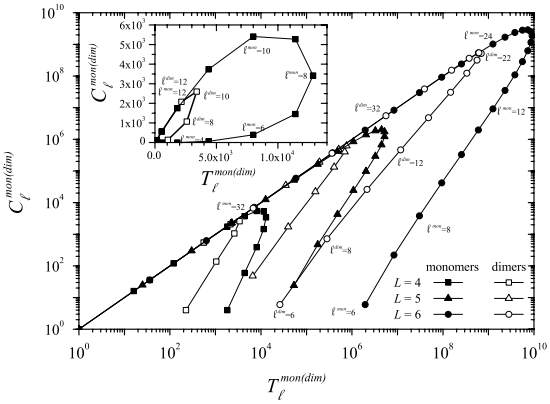

Fig. 2. Log–log curves of C_ℓ^{mon} versus T_ℓ^{mon} (solid symbols) and C_ℓ^{dim} versus T_ℓ^{dim} (open symbols) for three cell sizes (4×4, 5×5 and 6×6) and different values of length of the percolating trajectories as indicated. Each point in a given curve corresponds to a determined value of length of the percolating trajectory $\ell^{mon(dim)}$, as indicated. Inset: the case corresponding to the 4×4 cell is plotted on linear axes.

and (ii) for large values of ℓ, the number of percolating configurations is similar for monomers and dimers. Such behavior holds for different cell sizes.

For each curve which corresponds to a given cell size: (1) a maximum is clearly observed indicating the maximum number of percolating configurations of the cell, and (2) the values of these maxima are higher for monomers than for dimers. The two regimes described in the previous paragraph are also seen for each cell size. It is interesting to mention that during the second regime all the number of configurations C_ℓ^{mon} versus T_ℓ^{mon} (solid symbols) and C_ℓ^{dim} versus T_ℓ^{dim} (open symbols) lie on the same line to which all configurations with maximal percolating trajectories tend.

3. Results and discussion

By following the scheme presented in Section 2, the percolation function has been obtained for monomers and dimers deposited on cells of different sizes. To simplify the notation, we shall write $f_L^{mon}(p)$ and $f_L^{dim}(p)$ instead of $f_{\ell_{\min},\ell_{\max}}^{mon}(p)$ and $f_{\ell_{\min},\ell_{\max}}^{dim}(p)$, where $L = L_x = L_y$ for symmetric cells and $L = (L_x + L_y)/2$ for asymmetric cells. The results are shown in Fig. 3 (in this case, $L = 4$, 5 and 6). From a simple inspection of this figure it is observed that: (a) for a fixed size of depositing particle, the slope of the curves increases with increasing cell size. This effect allows us to make a finite-size scaling analysis in both systems (monomers and dimers); (b) the curves shift to lower values of p as the adsorbate changes from monomer to dimer. This finding, also observed from the maxima of $\lambda_L^{mon(dim)}(p) \equiv \frac{df_L^{mon(dim)}(p)}{dp}$ (see inset of Fig. 3), is a first indication that the percolation threshold of dimers is lower than the corresponding one for monomers. In the forthcoming subsections, the scaling properties of the percolation function will be used to estimate the critical parameters (percolation threshold and critical exponents ν, β and γ) corresponding to monomers and dimers on square lattices.

3.1. Exponent ν

As observed in Fig. 3, $f_L^{mon(dim)}(p)$ exhibits the typical behavior of an order parameter for the percolation transition. Then, as expected from the finite-size scaling theory [15–17,31–33],

$$f_L^{mon(dim)}(p) = \overline{f^{mon(dim)}}\left[(p - p_c)\, L^{1/\nu}\right], \tag{3}$$

being $\overline{f^{mon(dim)}}(u)$ the scaling function and $u \equiv (p - p_c)\, L^{1/\nu}$.

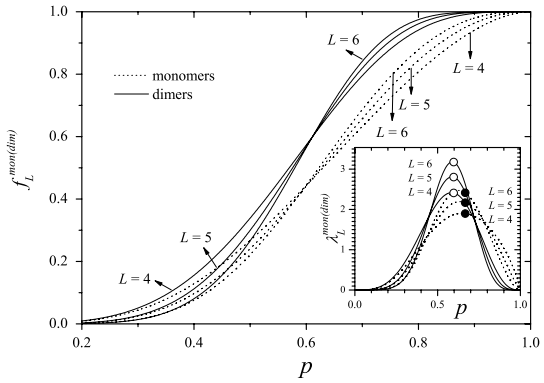

Fig. 3. Percolation functions and their derivatives (inset) versus concentration p for monomers and dimers deposited on cells of different sizes as indicated.

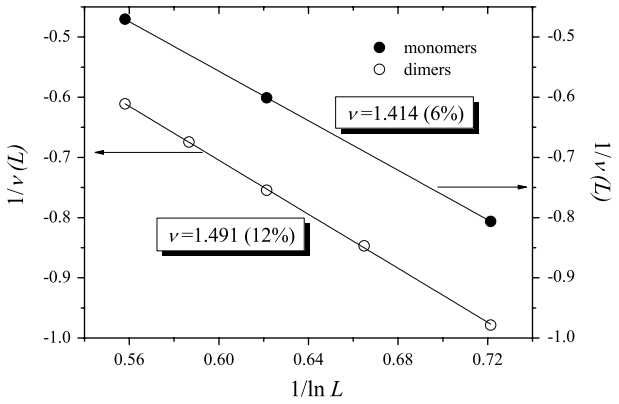

Fig. 4. Size dependence of the maximum value of the derivative of the percolation function used to determine ν. Full and open symbols correspond to monomers and dimers, respectively.

The derivative of this expression is

$$\frac{df^{mon(dim)}}{dp} = L^{1/\nu}\overline{f^{mon(dim)}}\left[(p - p_c)\, L^{1/\nu}\right], \tag{4}$$

which leads to

$$\frac{\ln\left[\frac{df_L^{mon(dim)}}{dp}\right]_{\max}}{\ln L} = \frac{1}{\nu}. \tag{5}$$

Reynolds et al. [34] proposed that, for small lattice sizes (as used here), Eq. (5) should be replaced by

$$\frac{\ln\left[\frac{df_L^{mon(dim)}}{dp}\right]_{\max}}{\ln L} = \frac{1}{\nu} - \frac{B}{\ln L}, \tag{6}$$

with B being a correction constant.

In Fig. 4, $\frac{\ln\left[df_L^{mon(dim)}/dp\right]_{\max}}{\ln L}$ has been plotted as a function of $1/\ln L$ for monomers and dimers as indicated. According to Eq. (6), the slope and intercept of each line correspond to B and $1/\nu$, respectively [35]. The results for ν from these fits are $\nu = 1.4140$ for monomers and $\nu = 1.4910$ for dimers, which differ by 6% and 12%, respectively, from the expected exact value $\nu = 4/3$ for ordinary percolation [13,14].

3.2. Percolation threshold and jamming coverage

The first step for determining the percolation threshold consists in evaluating the effective threshold $p_c(L)$ for a cell of finite size L. For this purpose, two procedures were applied, as described next.

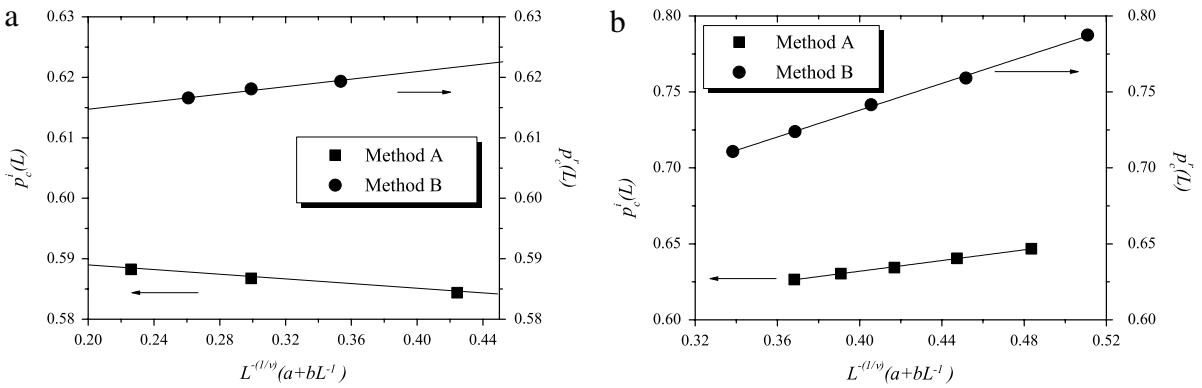

Fig. 5. Extrapolation of $p_c(L)$ towards the thermodynamic limit according to the theoretical prediction given by Eq. (7). Squares and circles denote the values of $p_c(L)$ obtained by using Methods A and B, respectively. (a) Data corresponding to monomers. (b) Data corresponding to dimers.

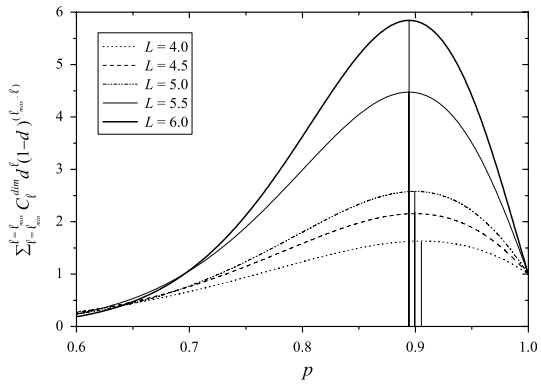

Fig. 6. Numerator in Eq. (2) $\left[\sum_{\ell=\ell_{\min}}^{\ell=\ell_{\max}} C_\ell^{dim} d^\ell (1-d)^{\ell_{\max}-\ell}\right]$ as a function of concentration p for dimers deposited on cells of different sizes as indicated.

Method A. The effective thresholds are obtained from the inflection points of the functions $f_L^{mon(dim)}(p)$, corresponding to the maxima of the first derivatives of the polynomial functions as shown in Fig. 3. The positions of these maxima will be designated by $p_c^i(L)$.

Method B. An alternative way of finding the effective percolation thresholds consists in using standard renormalization theory [2] and then solving the equation $f_L^{mon(dim)}(p) = p$ for the different lattice sizes. The values of concentration satisfying the last equation will be designated by $p_c^r(L)$.

Once the effective thresholds $p_c^{i(r)}(L)$ are obtained by Methods A and B, the percolation threshold in the thermodynamic limit, $p_c(\infty)$, is calculated by following the Reynolds scheme for small cells [7]:

$$p_c^{i(r)}(L) \approx p_c(\infty) + L^{-1/\nu}\left(a + bL^{-1} + cL^{-2} + dL^{-3} + \cdots\right), \tag{7}$$

where $a, b, c, \ldots$ are adjustable parameters.

Fig. 5 shows the extrapolation towards the thermodynamic limit of $p_c^{i(r)}(L)$ according to Eq. (7) and a correction of second order ($a, b \neq 0$ and $c, d, \ldots = 0$). Parts (a) and (b) present the results corresponding to monomers and dimers, respectively. The values obtained for monomers, $p_c^i(\infty) = 0.5926(2)$ and $p_c^r(\infty) = 0.5961(50)$, agree very well with recent calculations on classical site percolation (for a complete overview on this topic we refer the reader to Ref. [36]). In the case of dimers, the results obtained by both methods, $p_c^i(\infty) = 0.5616$ and $p_c^r(\infty) = 0.5617$, are consistent with previous simulation values [11,13,23,24].

On the other hand, it is interesting to analyze the behavior of the denominator (normalization factor) in Eq. (2). In the case of monomers, this term is equal to 1 (all sites have equal probability of being occupied). The situation is different for dimers, where the principle of equiprobability of occupation does not hold (see Fig. 2). Then, as can be seen in Fig. 6, when the function $\sum_{\ell=\ell_{\min}}^{\ell=\ell_{\max}} C_\ell^{dim} d^\ell (1-d)^{\ell_{\max}-\ell}$ (numerator in Eq. (2)) is plotted as a function of p, each curve corresponding to a given cell size presents a pronounced maximum at a concentration close to 0.8986. This value, which was obtained as an average over the five cell sizes indicated in the figure, accounts for the maximum number of particles that can be deposited on the lattice (the so-called jamming coverage θ_j). The result obtained here for θ_j is in excellent agreement with previous published results: $\theta_j = 0.90668$ [13], $\theta_j = 0.906$ [23] and $\theta_j = 0.907$ [24].

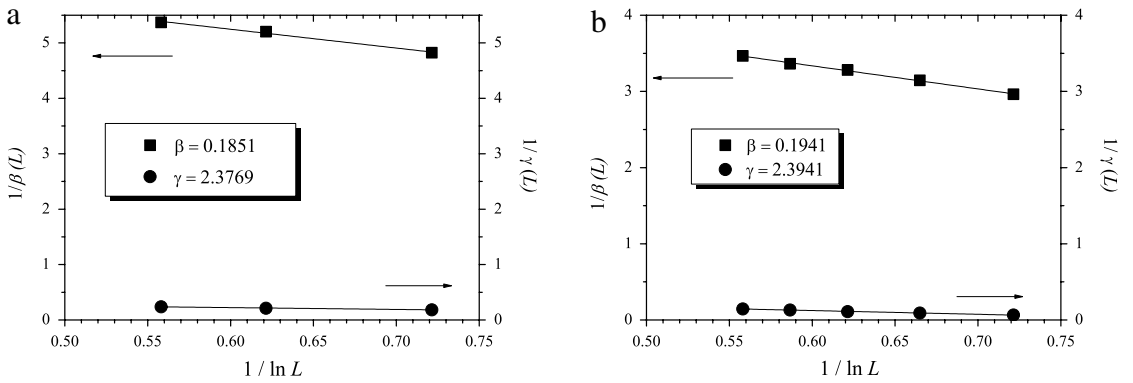

Fig. 7. Linear fittings used to determine β (squares) and γ (circles). (a) Data corresponding to monomers. (b) Data corresponding to dimers.

Table 3
Comparison of published and present results for percolation of dimers on square lattices.

Critical parameters	This work	Previous work
p_c	$0.5616(p_c^i)$, $0.5617(p_c^r)$	0.5618(2) [11], 0.5617 [13], 0.562 [24], 0.562(3) [25]
θ_j	0.8986	0.90668 [13], 0.906 [24], 0.907(3) [25]
ν	1.491	4/3 [2], 1.368(24) and 1.373(23) [14]
β	0.1941	5/36 [2], 0.179(2) [13], 0.121(13) [14]
γ	2.3941	43/18 [2], 2.37(5) [13], 2.452(13) [14]

3.3. Exponents β and γ

The strength or weight of the percolating cluster P vanishes at the transition and is non-analytic,

$$P \sim |p - p_c|^{\beta}, \tag{8}$$

defining the exponent β. Here, P plays the role of an order parameter. On the other hand, the divergence of the mean cluster size,

$$S = \sum_s \frac{s^2 n_s}{p_c} \sim |p - p_c|^{\gamma}, \tag{9}$$

introduces the exponent γ.

In order to determine these critical exponents, it must be considered that the parameters P and S can be expressed as a function of $f^{dim}_{\ell_{\min},\ell_{\max}}(d)$ in the interval $p > p_c$ and $p < p_c$, respectively. Thus, the critical exponents obtained for each cell size, $\beta(M)$ and $\gamma(M)$, are plotted as function of the inverse of the minimum percolation length in Fig. 7 [35,37]. In the figure, identical correction criteria as in Fig. 4 are used. A nearly linear tendency is clearly observed in Fig. 7(a) (monomers) and Fig. 7(b) (dimers). Note that in the figure both symmetrical and asymmetrical cells have been included. Thus, the tendency to the thermodynamic limit determines the values of the critical exponents: (i) $\beta = 0.1851$ and $\gamma = 2.3769$ for monomers, and (ii) $\beta = 0.1941$ and $\gamma = 2.3941$ for dimers. In both cases, the reported values of β and γ are in agreement with expected results [13,14].

Finally, Table 3 summarizes the results obtained for dimers in the present work in comparison to previously published results using simulation techniques. In the case of ν, β and γ, the table also includes the exact expected theoretical values given as rational numbers.

4. Conclusions

In this work, percolation of homonuclear dimers on square lattices has been studied by using a theoretical approach, which is based on the exact calculation of configurations on finite rectangular cells. An efficient algorithm allows us to calculate the detailed structure of the configuration space for $M = L_x \times L_y$ cells, with M varying from 16 to 36.

From the counting of the number of configurations leading to percolation (normalized over a term involving the number of available configurations for dimers on the cell), the percolating function $f_L^{dim}(p)$ was introduced. Taking advantage of its definition, the percolation threshold, jamming coverage and critical exponents were calculated.

In the case of p_c, two methods have been used. In the first, the percolation threshold is obtained from extrapolation towards the thermodynamic limit of the positions of the inflection points of the percolation function curves. In the second, the percolation threshold is determined from the well-known renormalization equation $f_L^{dim}(p) = p$. The values of p_c

calculated by both methods are in excellent agreement with previous simulation data reported in the literature [11,13,23,24].

On the other hand, the maximum number of particles that can be deposited on the lattice was calculated by analyzing the behavior of the numerator of $f_L^{dim}(p)$. For each cell size, the corresponding curve presents a pronounced maximum at a concentration close to 0.8986. This value of θ_j is in excellent agreement with previous published results [13,23,24].

With respect to the critical exponents for dimers, the results reported here for ν, β and γ (1) differ by 12%, 40% and 0.2%, respectively, from the expected exact values $\nu = 4/3$, $\beta = 5/36$ and $\gamma = 43/18$ for ordinary percolation; and (2) are in general good agreement with previous published data [13,14].

The extension of the method to other geometries and adsorbate structures will be the object of future studies.

Acknowledgments

W.L. and J.F.V. are grateful for support from the Universidad de la Frontera (Temuco, Chile) under project DIUFRO, DI11-0031. F.N. and A.J.R.P. are grateful for support from the Universidad Nacional de San Luis (Argentina) under project 322000, CONICET (Argentina) under project PIP 112-200801-01332 and the National Agency of Scientific and Technological Promotion (Argentina) under project PICT-2010-1466. Partial support from FONDECYT (Chile) under project 1100156, Millennium Scientific Nucleus "Basic and Applied Magnetism" and Center for the Development of Nanoscience and Nanotechnology is also acknowledged.

References

[1] R. Zallen, The Physics of Amorphous Solids, Willey & Sons, New York, 1983.
[2] D. Stauffer, A. Aharony, Introduction to Percolation Theory, second ed., Taylor & Francis, London, 1994.
[3] M. Sahimi, Applications of Percolation Theory, Taylor & Francis, London, 1994; Flow and Transport in Porous Media and Fractured Rock, VCH, Weinheim, Germany, 1995.
[4] G. Grimmett, Percolation, Springer-Verlag, Berlin, 1999.
[5] B. Bollobás, O. Riordan, Percolation, Cambridge University Press, New York, 2006.
[6] M.E.J. Newman, R.M. Ziff, Phys. Rev. Lett. 85 (2000) 4104.
[7] P.M.C. de Oliveira, R.A. Nóbrega, D. Stauffer, Braz. J. Phys. 33 (2003) 616.
[8] M.J. Lee, Phys. Rev. E 76 (2007) 027702.
[9] X. Feng, Y. Deng, H.W.J. Blöte, Phys. Rev. E 78 (2008) 031136.
[10] M.J. Lee, Phys. Rev. E 78 (2008) 031131.
[11] Y. Leroyer, E. Pommiers, Phys. Rev. B 50 (1994) 2795.
[12] Z. Gao, Z.R. Yang, Physica A 255 (1998) 242.
[13] V.A. Cherkasova, Y.Y. Tarasevich, N.I. Lebovka, N.V. Vygornitskii, Eur. Phys. J. B 74 (2010) 205.
[14] V. Cornette, A.J. Ramirez-Pastor, F. Nieto, Eur. Phys. J. B 36 (2003) 391.
[15] A.M. Ferrenberg, D.P. Landau, Phys. Rev. B 44 (1991) 5081.
[16] W. Janke, M. Katoot, R. Villanova, Phys. Rev. B 49 (1994) 9644.
[17] K. Binder, E. Luijten, Phys. Rep. 344 (2001) 179.
[18] M. Aizenman, Nuclear Phys. B 485 (1997) 551.
[19] J. Cardy, J. Phys. A 31 (1998) L105.
[20] L.N. Shchur, S.S. Kosyakov, Int. J. Mod. Phys. C 8 (1997) 473.
[21] L.N. Shchur, in: D.P. Landau, S.P. Lewis, H.B. Schuettler (Eds.), Incipient Spanning Clusters in Square and Cubic Percolation, in: Springer Proceedings in Physics, vol. 85, Springer Verlag, Heidelberg, Berlin, 2000.
[22] J.W. Evans, Rev. Modern Phys. 65 (1993) 1281.
[23] N. Vandewalle, S. Galam, M. Kramer, Eur. Phys. J. B 14 (2000) 407.
[24] M. Dolz, F. Nieto, A.J. Ramirez-Pastor, Eur. Phys. J. B 43 (2005) 363.
[25] H.S. Choi, J. Talbot, G. Tarjus, P. Viot, Phys. Rev. E 51 (1995) 1353.
[26] M. Porto, H.E. Roman, Phys. Rev. E 62 (2000) 100.
[27] G. Kondrat, A. Pekalski, Phys. Rev. E 63 (2001) 051108; Phys. Rev. E 64 (2001) 056118.
[28] F. Rampf, E.V. Albano, Phys. Rev. E 66 (2002) 061106.
[29] E.S. Loscar, R.A. Borzi, E.V. Albano, Phys. Rev. E 68 (2005) 041106.
[30] P. Danwanichakul, E.D. Glandt, J. Colloid Interface Sci. 283 (2005) 41.
[31] R.M. Ziff, M.E.J. Newman, Phys. Rev. E 66 (2002) 016129.
[32] A. Rosowsky, Eur. Phys. J. B 15 (2000) 77.
[33] C. Tsallis, A. Coniglio, G. Schwachheim, Phys. Rev. B 32 (1985) 3322.
[34] P.J. Reynolds, H.E. Stanley, W. Klein, Phys. Rev. B 21 (1980) 1223.
[35] W. Lebrecht, M.I. González, Rev. Mexicana Fís. 57 (4) (2011) 344.
[36] M.J. Lee, Phys. Rev. E 78 (2008) 031131.
[37] E.E. Vogel, W. Lebrecht, J.F. Valdés, Physica A 389 (2010) 1512.